articles

molecular pharmaceutics

Nanoscaled Polyion Complex Micelles for Targeted Delivery of Recombinant Hirudin to Platelets Based on Cationic Copolymer

Fei Wang,[†,‡] Xinru Li,[†,‡] Yanxia Zhou,[†] Yanhui Zhang,[†] Xingwei Chen,[†] Jingxiong Yang,[†] Yanqing Huang,[§] and Yan Liu*[,†]

Department of Pharmaceutics, School of Pharmaceutical Sciences, Peking University, Beijing 100191, China, and Pharmaceutical Teaching Laboratory Center, Peking University, Beijing 100191, China

Received November 2, 2009; Revised Manuscript Received February 8, 2010; Accepted March 29, 2010

Abstract: Polyion complex (PIC) micelles based on methoxy poly(ethylene glycol)-grafted-chitosan (mPEG-*g*-chitosan) and Arg-Gly-Asp conjugated poly(ethylene glycol)-grafted-chitosan (RGD−PEG-*g*-chitosan) were designed as carriers for platelet-targeted delivery of recombinant hirudin variant-2 (rHV2). The rHV2-loaded plain PIC micelles (mPIC micelles) and RGD conjugated PIC micelles (RGD−PIC micelles) were successfully prepared with mean size of 30.9 ± 0.5 nm and 41.9 ± 1.8 nm, and their encapsulation efficiencies were 76.90 ± 0.84% and 81.08 ± 0.85%, respectively. The pharmacokinetics experiments showed that the mean retention time (MRT) of rHV2 encapsulated in both kinds of micelles was significantly prolonged, especially for mPIC micelles. The confocal laser scanning microscopy intuitively proved the specific binding of RGD−PIC micelles to platelets. The efficacies of rHV2-loaded RGD−PIC micelles were greatly better than those of rHV2-loaded mPIC micelles and rHV2 solution in aspect of anticoagulation and inhibition of platelet aggregation. These results suggested platelet-targeting specificity of RGD−PIC micelles and that RGD−PIC micelles could potentially be used as a carrier for platelet-targeted delivery and long circulation of rHV2.

Keywords: Recombinant hirudin; polyion complex micelles; platelet-targeted; poly(ethylene glycol)-grafted-chitosan; anticoagulant activity; inhibition of platelet aggregation

Introduction

Hirudin has become the most specific tight-binding thrombin inhibitor since it was isolated in the late 1950s,[1] and it has been applied in the clinic to treat acute coronary artery disease,[2] deep vein thrombosis,[3] and disseminated intravascular coagulation[4] due to its lower side effects of hemorrhage and nonallergic reaction and nontoxicity[5] compared with heparin. Although hirudin is a promising anticoagulant, it also has some drawbacks. Clinical pharmacokinetic studies of hirudin performed in human volunteers showed that hirudin was rapidly distributed into the extracellular space after intravenous injection and eliminated with a half-life of 60−100 min.[6] Hence, repeated injections are

* Corresponding author. Mailing address: Department of Pharmaceutics, School of Pharmaceutical Sciences, Peking University, Xueyuan Road 38, Beijing 100191, China. Phone: 86-10-82801508. Fax: 86-10-62015584. E-mail: yanliu@bjmu.edu.cn.

† Department of Pharmaceutics, School of Pharmaceutical Sciences.

‡ These authors contributed equally to this work.

§ Pharmaceutical Teaching Laboratory Center.

(1) Matheson, A. J.; Goa, K. L. Desirudin: a review of its use in the management of thrombotic disorders. *Drugs* **2000**, *60*, 679–700.

(2) Zoldhelyi, P.; Webster, M. W. I.; Fuster, V.; Grill, D. E.; Gaspar, D.; Edwards, S. J.; Cabot, C. F.; Chesebro, J. H. Recombinant hirudin in patients with chronic, stable coronary artery disease: safety, half-life and effect on coagulation parameters. *Circulation* **1993**, *88*, 2015–2022.

(3) Levinand, L. A.; Bergqvist, D. Cost effectiveness of desirudin compared with a low molecular weight heparin in the prevention of deep vein thrombosis after total hip replacement surgery. *PharmacoEconomics* **2001**, *19*, 589–597.

10.1021/mp900271r
Published on Web 03/29/2010

required due to the rapid clearance of hirudin from the circulation. Considering the high price of hirudin, the therapy becomes more expensive. Moreover, repeated injections may be potentially life-threatening and unsafe for patients.[7] These disadvantages have significantly limited the clinical application of hirudin.[8−10] Consequently, recent efforts have been directed to the development of drug delivery systems to solve the problems referred to. Attempts at other administration routes have been made, such as thermosensitive hydrogel for the controlled release of hirudin by subcutaneous administration,[11] chitosan/polyethylene glycol-alginate microcapsules for oral delivery of hirudin,[12] and nasal spray with chitosan enhancer.[13] Although the residence time of hirudin in blood was prolonged for these administration routes, the absolute bioavailability was still lower, and large amounts of organic solvents used during preparation of formulation such as microcapsules were a knotty problem as well. Hence, there has been an urgent request to develop an efficient and adequate vehicle that can carry and deliver hirudin to the intended site without provoking any adverse reaction.

Among the many exciting nanoplatforms such as polymeric micelles and dendrimers, polyion complex micelles (PIC micelles) provide a complementary yet unique nanocarrier system and have attracted much attention in recent years.[14−17] PIC micelles generally result from cooperative electrostatic interactions between a charged copolymer and an oppositely charged species.[18] The formation of PIC micelles is best described as the sequential complexation of a charged polymer and an oppositely charged species through electrostatic interactions followed by the self-association of the condensates into micelles. Neutralization of the charged segments indeed yields water-insoluble moieties that contribute to a decrease in the entropy of the system. To offset this entropy loss, the neutralized segments withdraw from the aqueous phase and self-assemble into micelles presenting a core−shell architecture. The charge-compensated anionic drug/cationic chains self-assemble into a micellar core while the hydrophilic segments form a protecting corona.[19] The corona not only confers solubility and colloidal stability to the system but also shields any cationic charges. Complexes with surface cationic charges are known to unspecifically interact with blood components and nontarget cells, leading to short blood half-life and toxicity when *in vivo* applications are sought.[20] Therefore, PIC micelles exhibit numerous superiorities such as small size with narrow distribution, long circulation, especially, high entrapment efficiency, and self-assembly in aqueous medium. In use of PIC micelles, nucleic acid drugs,[21−23] peptides and proteins[24,25] and anionic drugs[15] have been successfully incorporated in the core of micelles. Only a few kinds of polymers have been used as cationic segment, including poly(L-lysine),[26] poly(dimethylaminoethyl methacrylate),[22] poly(ethylenimine),[23] chitosan[15] and so on. Among these cationic polymers, only chitosan is the best candidate due to its relatively good biocompatibility, biodegradability, low immunogenicity, nontoxicity, natural source and low price. Poly(ethylene glycol) (PEG) is frequently chosen as a hydrophilic segment because it is biocompatible and possible to provide steric stabilization of

(4) José, H.; Ramón, M.; José Antonio, P.; Eduardo, R. Endotoxin-induced disseminated intravascular coagulation in rabbits: Effect of recombinant hirudin on hemostatic parameters, fibrin deposits, and mortality. *J. Lab. Clin. Med.* **1998**, *131*, 77–83.

(5) Markwardt, F. The development of hirudin as an antithrombotic drug. *Thromb. Res.* **1994**, *74*, 1–23.

(6) Kim, D. D.; Horbett, T. A.; Takeno, M. M.; Ratner, B. D. Pharmacology and controlled release of hirudin for cardiovascular disorders. *Cardiovasc Pathol.* **1996**, *5*, 337–349.

(7) Wathion N. EMEA public statement on refludan (lepirudin). http://www.emea.eu.intJpdfs/human/press/pus/277 1702en.pdf (2002).

(8) Rydel, T. J.; Ravichandran, K. G.; Tulinsky, A.; Bode, W.; Huber, R.; Roitsch, C.; Fenton, J. W. Structure of a complex of recombinant hirudin and human α-thrombin. *Science* **1990**, *249*, 277–280.

(9) Rydel, T. J.; Tulinsky, A.; Bode, W.; Huber, R. Refined structure of the Hirudin-thrombin complex. *J. Mol. Biol.* **1991**, *221*, 583–601.

(10) Markwardt, F. Past, present and future of hirudin. *Haemostasis* **1991**, *21* (Suppl 1), 11–26.

(11) Liu, Y.; Lu, W. L.; Wang, J. C.; Zhang, X.; Zhang, H.; Wang, X. Q.; Zhou, T. Y.; Zhang, Q. Controlled delivery of recombinant hirudin based on thermo-sensitive Pluronic® F127 hydrogel for subcutaneous administration: In vitro and in vivo characterization. *J. Controlled Release* **2007**, *117*, 387–395.

(12) Chandy, T.; Mooradian, D. L.; Rao, G. H. R. Chitosan/polyethylene glycol-alginate microcapsules for oral delivery of hirudin. *J. Appl. Polym. Sci.* **1998**, *70*, 2143–2153.

(13) Zhang, Y. J.; Ma, C. H.; Lu, W. L.; Zhang, X.; Wang, X. L.; Sun, J. N.; Zhang, Q. Permeation-enhancing effects of chitosan formulations on recombinant hirudin-2 by nasal delivery in vitro and in vivo. *Acta Pharmacol. Sin.* **2005**, *26*, 1402–1408.

(14) Prego, C.; Torres, D.; Fernandez-Megia, E.; Novoa-Carballal, R.; Quiñoá, E.; Alonso, M. J. Chitosan-PEG nanocapsules as new carriers for oral peptide delivery: Effect of chitosan pegylation degree. *J. Controlled Release* **2006**, *111*, 299–308.

(15) Yang, K. W.; Li, X. R.; Yang, Z. L.; Li, P. Z.; Wang, F.; Liu, Y. Novel polyion complex micelles for liver-targeted delivery of diammonium glycyrrhizinate:in vitro and in vivo charcterization. *J. Biomed. Mater. Res. A* **2009**, *88*, 140–148.

(16) Bhattarai, N.; Ramay, H. R.; Gunn, J.; Matsen, F. A.; Zhang, M. PEG-grafted chitosan as an injectable thermosensitive hydrogel for sustained protein release. *J. Controlled Release* **2005**, *103*, 609–624.

(17) Zhang, X.; Zhang, H.; Wu, Z.; Wang, Z.; Niu, H.; Li, C. Nasal absorption enhancement of insulin using PEG-grafted chitosan nanoparticles. *Eur. J. Pharm. Biopharm.* **2008**, *68*, 526–534.

(18) Kataoka, K.; Harada, A.; Nagasaki, Y. Block copolymer micelles for drug delivery: design, characterization and biological significance. *Adv. Drug Delivery Rev.* **2001**, *47*, 113–131.

(19) Kataoka, K.; Togawa, H.; Harada, A.; Yasugi, K.; Matsumoto, T.; Katayose, S. Spontaneous Formation of Polyion Complex Micelles with Narrow Distribution from Antisense Oligonucleotide and Cationic Block Copolymer in Physiological Saline. *Macromolecules* **1996**, *29*, 8556–8557.

(20) Ogris, M.; Brunner, S.; Schüller, S.; Kircheis, R.; Wagner, E. PEGylated DNA/transferrin-PEI complexes: reduced interaction with blood components, extended circulation in blood and potential for systemic gene delivery. *Gene Ther.* **1999**, *6*, 595–605.

the micelles. Furthermore, pegylation can also increase the circulation time of the drug in the blood by masking it from recognition by the reticuloendothelial system.[27] Our previous study also revealed that PEG-grafted-chitosan would be a new kind of polymer for preparing PIC micelles.[15]

Herein, we reported the development of PIC micelles that targeted platelets. The micelle surface was functionalized with a platelet-targeting peptide, Arg-Gly-Asp (RGD), which is membrane integrin acceptor and can be recognized by activated-platelet globulin protein (GP) IIb/IIIa.[28] mPEG-*g*-chitosan and RGD−PEG-*g*-chitosan were synthesized and characterized. The rHV2-loaded PIC micelles with both long-circulation and platelet-targeted functions were developed based on mPEG-*g*-chitosan and RGD−PEG-*g*-chitosan, their physicochemical characteristics were investigated, and the pharmacokinetics of rHV2-loaded PIC micelles in rats after intravenous administration was evaluated in comparison with rHV2 solution. The platelet-targeting specificity of rHV2-loaded PIC micelles was systematically examined.

Experimental Section

Chemicals. Poly(ethylene glycol) (PEG) and methoxy poly(ethylene glycol) (mPEG) with M_w 2 kDa were obtained from Sigma (St. Louis, MO). Chitosan with deacetylation degree of 78.05% and M_w 40 kDa was provided by Goldenshell Biochemical Co. Ltd. (Zhejiang, China). Cyanoborohydride ($NaBH_3CN$) and fluorescein isothiocyanate (FITC) were purchased from Sigma (St. Louis, MO). Recombinant hirudin variant-2 (rHV2, 5000 ATU/mg) was obtained from College of Life Science, Peking University (Beijing, China). Pentasodium tripolyphosphate (TPP) was supplied by Tianfu (Jiangsu, China). Arg-Gly-Asp peptide (RGD) was purchased from C-Strong Co. Ltd. (Shanghai, China). Kits for determination of protein concentration were purchased from Bio Cellchip Co. Ltd. (Beijing, China). Kits for determining activated partial thromboplasmin time (APTT) were obtained from Sun Biotech Co. Ltd. (Shanghai, China). Adenosine diphosphate (ADP) was purchased from Steellex Co. Ltd. (Beijing, China). All other chemicals were of reagent grade.

Animals. Male Sprague−Dawley (SD) rats weighing 200 ± 20 g were obtained from Experimental Animal Center of Peking University, and acclimatized for 7 days after arrival. Male New Zealand white rabbits weighing 2.5 ± 0.2 kg were purchased from the same supplier and acclimatized for 2 days after arrival. All animals were provided with standard food and water ad libitum, and were exposed to alternating 12 h periods of light and darkness. Temperature and relative humidity were maintained at 25 °C and 50%, respectively. All care and handling of animals were performed with the approval of Institutional Authority for Laboratory Animal Care.

Polymer Synthesis and Characterization. mPEG-CHO or CHO-PEG-CHO was prepared by oxidation of mPEG or PEG with DMSO/acetic anhydride according to the previous report[29] with little modification. Briefly, 10 g of mPEG or PEG was dissolved in 40 mL of anhydrous DMSO, followed by addition of 10 mL of acetic anhydride. The molar ratio of acetic anhydride to PEG was 10:1. The resultant mixture was stirred for 8 h at room temperature under a nitrogen atmosphere and then precipitated with excess diethyl ether. After drying under vacuum, white powder of mPEG-CHO or CHO-PEG-CHO was obtained. The conversion degree from hydroxy group to aldehyde group was determined by the $NaHSO_3$ method.[30]

mPEG-*g*-chitosan was prepared by alkylation of chitosan followed by Schiff base formation according to the previous report.[31] mPEG-CHO and chitosan with a molar ratio of 1:20 were added into acetate buffer solution at pH 4.6 under stirring. After 24 h, $NaBH_3CN$ was added dropwise into the resulting mixture with a molar ratio of 1:1 for mPEG-CHO

(21) Kakizawa, Y.; Kataoka, K. Block copolymer micelles for delivery of gene and related compounds. *Adv Drug Delivery Rev.* **2002**, *54*, 203–222.

(22) Wakebayashi, D.; Nishiyama, N.; Yamasaki, Y.; Itaka, K.; Kanayama, N.; Harada, A.; Nagasaki, Y.; Kataoka, K. Lactose-conjugated polyion complex micelles incorporating plasmid DNA as a targetable gene vector system: their preparation and gene transfecting efficiency against cultured HepG2 cells. *J. Controlled Release* **2004**, *95*, 653–664.

(23) Tian, H.; Deng, C.; Lin, H.; Sun, J.; Deng, M.; Chen, X.; Jing, X. Biodegradable cationic PEG-PEI-PBLG hyperbranched block copolymer: synthesis and micelle characterization. *Biomaterials* **2005**, *26*, 4209–4217.

(24) Harada, A.; Kataoka, K. Novel Polyion Complex Micelles Entrapping Enzyme Molecules in the Core: Preparation of Narrowly-Distributed Micelles from Lysozyme and Poly(ethylene glycol)-Poly(aspartic acid) Block Copolymer in Aqueous Medium. *Macromolecules* **1998**, *31*, 288–294.

(25) Dufresne, M. H.; Leroux, J. C. Study of the Micellization Behavior of Different Order Amino Block Copolymers with Heparin. *Pharm. Res.* **2004**, *21*, 160–169.

(26) Jang, W. D.; Nakagishi, Y.; Nishiyama, N.; Kawauchi, S.; Morimoto, Y.; Kikuchi, M.; Kataoka, K. Polyion complex micelles for photodynamic therapy: Incorporation of dendritic photosensitizer excitable at long wavelength relevant to improved tissue-penetrating property. *J. Controlled Release* **2006**, *113*, 73–79.

(27) Moghimi, S. M.; Hunter, A. C.; Murray, J. C. Long-circulating and target-specific nanoparticles: theory to practice. *Pharmacol. Rev.* **2001**, *53*, 283–318.

(28) Nicholson, N. S.; Panzer-Knodle, S. G.; Salyers, A. K.; Taite, B. B.; King, L. W.; Miyano, M.; Gorczynski, R. J.; Williams, M. H.; Zupec, M. E.; Tjoeng, F. S. Antiplatelet and antithrombotic effects of platelet glycoprotein IIb/IIIa (GP IIb/IIIa) inhibition by arginine-glycine-aspartic acid- serine (RGDS) and arginine-glycine-aspartic acid (RGD) (O-me)Y (SC- 46749). *Pharmcology* **1991**, *256*, 876–882.

(29) Muslim, T.; Morimoto, M.; Saimoto, H.; Okamoto, Y.; Minami, S.; Shigemasa, Y. Synthesis and bioactivities of poly(ethylene glycol)-chitosan hybrids. *Carbohydr. Polym.* **2001**, *46*, 323–330.

(30) Vogel, A. I.; Tatchell, A. R.; Furnis, B. S.; Hannaford, A. J. Smith, P. W. G. *Vogel's Textbook of Practical Organic Chemistry*, 5th ed.; Prentice Hall: London, 1989; p 1220.

(31) Harris, J. M.; Struck, E. C.; Case, M. G.; Paley, M. S.; Yalpani, M. J.; Van Alstine, M.; Brooks, D. E. Synthesis and characterization of poly(ethylene glycol) derivatives. *J. Polym. Sci., Polym. Chem. Ed.* **1984**, *22*, 341–352.

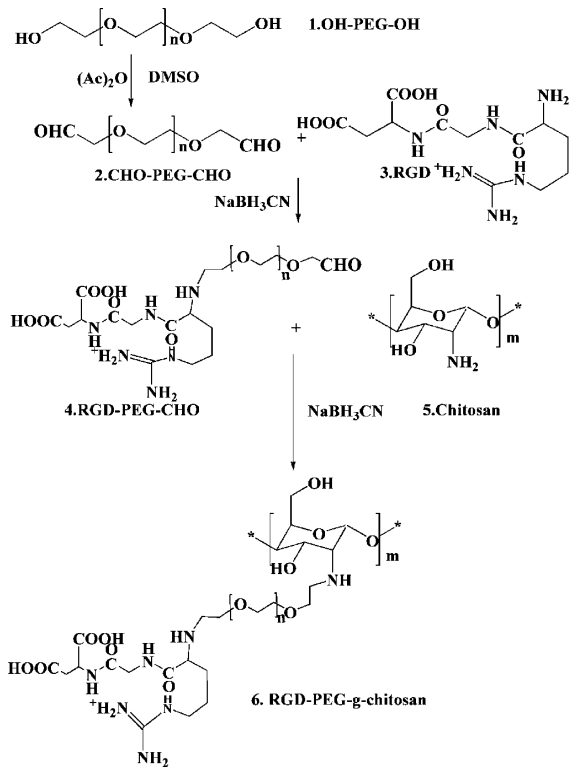

Figure 1. Scheme for synthesis of RGD−PEG-*g*-chitosan.

and $NaBH_3CN$. The resultant mixture was dialyzed with a dialysis membrane (MW cutoff = 12−14 kDa, Millipore Co. Ltd., USA) against distilled water, and the solution was subsequently freeze-dried. mPEG-*g*-chitosan was obtained by removal of residuary mPEG-CHO from the freeze-dried samples with excess acetone. The final product was dissolved in D_2O, and then the ^1H NMR spectrum was recorded on a Bruker MSL2300 spectrometer (300 MHz, Germany) using tetramethylsilane (TMS) as an internal reference at room temperature. The FTIR spectra of the final product and chitosan were recorded with KBr pellets on an AVATAR360 spectrophotometer (Nicolet, USA). The grafting degree of chitosan was measured by the TNBS method.[32]

RGD−PEG-*g*-chitosan was synthesized according to the previous reports[15,33] with little modification. The synthetic scheme was shown in Figure 1. CHO-PEG-CHO and RGD with a molar ratio of 1:0.5 were dissolved in 95% alcohol at pH 4.6 (adjusted with acetate solution) under stirring for 24 h. Then $NaBH_3CN$ was added dropwise into the above mixture with a molar ratio of 1:0.5 for CHO-PEG-CHO and $NaBH_3CN$. The resultant mixture was dialyzed with a dialysis membrane (MW cutoff = 1 kDa, Millipore Co. Ltd., USA) against distilled water, and the solution was subsequently freeze-dried. CHO-PEG-RGD was obtained, and the linkage of RGD with CHO-PEG-CHO was supported by nitrogen element analysis. The following steps were the same as those described in the synthesis of mPEG-*g*-chitosan, and then RGD−PEG-*g*-chitosan was obtained by removal of the residue RGD−PEG-CHO from the freeze-dried samples with excess acetone. The linkage of RGD−PEG-CHO with chitosan was supported by thin layer chromatography (TLC, developing solvent: *n*-butanol/water/acetic acid = 4/1/1, ninhydrin as chromogenic agent) of the hydrolysis sample of the final product in 6 mol/L hydrochloric acid compared with the hydrolysis product of free RGD. The FTIR spectra of the final product and chitosan were recorded as described above. Similarly, the grafting degree of chitosan was measured by the TNBS method.

Preparation and Physicochemical Characterization of rHV2-Loaded PIC Micelles. The PIC micelles were prepared as previously described.[14] Briefly, mPEG-*g*-chitosan or RGD−PEG-*g*-chitosan solution (1.6 mg/mL) was prepared by dissolving mPEG-*g*-chitosan or RGD−PEG-*g*-chitosan in acetate buffer (pH 5.0, 1%), and then mixed with equal volume of 0.2 mg/mL rHV2 solution. Under magnetic stirring at room temperature, 2 mL of TPP solution (1.1 mg/mL) was added into 5 mL of the resulting solution drop by drop at a speed of 0.1 mL/min controlled by a peristaltic pump (Lange BT-300-300M, China). After the addition, the solution was kept stirring for 30 min to obtain rHV2-loaded PIC micelles. After micelle production, the micelle size and size distribution (polydispersity index, PDI) were measured by the dynamic light scattering (DLS) method (Malvern Zetasizer ZEN3500, U.K.). All DLS measurements were performed at a wavelength of 532 nm with a scattering angle of 173° at 25 °C. The results were the mean values of three experiments for the same sample. Zeta potential was also determined by this instrument. The encapsulation efficiency (EE) was calculated as the percentage of loaded rHV2 over the original feeding amount of rHV2 as described below. The rHV2-loaded PIC micelles were ultrafiltered with a filtration membrane of molecular weight cutoff of 10 kDa (Millipore Co. Ltd., USA), and the rHV2 concentration in the ultrafiltrate was determined by commercially available kits following the instruction for corresponding kits.[34] The encapsulation efficiency (EE) was calculated as follows:

$$\mathrm{EE} = \frac{\text{total amount of rHV2} - \text{amount of free rHV2}}{\text{total amount of rHV2}} \times 100\%$$

wherein amount of free rHV2 = the total volume of micelle solution before ultrafiltration × rHV2 concentration in the ultrafiltrate.

(32) Ye, Y. Q.; Yang, F. L.; Hu, F. Q.; Du, Y. Z.; Yuan, H.; Yu, H. Y. Core-modified Chitosan based Polymeric Micelles for Controlled Release of Doxorubicin. *Int. J. Pharm.* **2008**, *352*, 294–301.

(33) Hu, Y.; Jiang, H.; Xu, C.; Wang, Y.; Zhu, K. Preparation and characterization of poly(ethylene glycol)-g-chitosan with water- and organosolubility. *Carbohydr. Polym.* **2005**, *61*, 472–479.

(34) Yu, Q.; He, J. T.; Mo, W.; Zhang, Y. L.; Wang, L. S.; Wu, Y. Z.; Song, H. Y. Preparation and characterization of poly(lactic-co-glycolic acid) microspheres containing RGD-hirudin. *Fudan Univ. J. Med. Sci.* **2006**, *33*, 17–23.

Preparation of FITC-Labeled rHV2. rHV2 was labeled with FITC according to the previous report.[35] Briefly, 100 μL of carbonate buffer solution (pH 9.0, 100 mmol/L) with 1.06 mg of FITC was added to 1 mL of carbonate buffer solution (pH 9.0, 100 mmol/L) containing 20 mg/mL of rHV2 under gently stirring. The reaction was continued for 4 h at room temperature in the dark. Then FITC labeled rHV2 (FITC-rHV2) was obtained after the free FITC was removed by gel chromatography through Sephadex G-25 gel column.

Pharmacokinetics of rHV2-Loaded PIC Micelles. Three groups of SD rats (five ones per group) were used to evaluate the pharmacokinetics of rHV2 formulations as follows: (1) FITC-rHV2 solution, (2) FITC-rHV2-loaded mPIC micelles, (3) FITC-rHV2-loaded RGD−PIC micelles. All rHV2 formulations (containing 0.2 mg/mL rHV2) were given intravenously to rats by tail vein at a dose of 2 mg/kg. 0.5 mL blood samples for determining the concentration of FITC-rHV2 were collected under anesthesia from the orbital sinus at predetermined time intervals. The plasma was collected by centrifugation at 2000*g* for 10 min and stored at −20 °C until analysis. The plasma concentration of FITC-rHV2 was determined by fluorescence spectrophotometer.[36] The pharmacokinetic parameters associated with each group were assessed by WinNonLin (Pharsight, Mountain View, CA) using noncompartmental analysis. The initial plasma FITC-rHV2 concentration (C_0), mean residence time up to last time (MRT_{0-t}), and area under the plasma concentration−time curve up to last time (AUC_{0-t}) for each rat were obtained.

Anticoagulant Activity Assay. Anticoagulant activity of rHV2 formulations was evaluated by measuring activated partial thromboplastin time (APTT). SD rats were used to evaluate the pharmacological efficacy of rHV2-loaded PIC micelles. Blank blood samples for evaluation of clotting times were collected under anesthesia from the orbital sinus and placed in tubes containing 3.8% (w/v) sodium citrate solution (1.75:10, v/v, for sodium citrate solution and blood).[37] To 300 μL of blood, 30 μL of each rHV2 formulation with different concentration of rHV2 was added. Then the mixture was incubated at 37 °C for 20 min and centrifuged at 2000*g* for 10 min. The plasma obtained was analyzed immediately. The APTT for each sample was determined by commercially available APTT kits according to the instruction for corresponding kits. The prolongation of APTT compared with corresponding initial values of blank blood for each rat was considered to reflect the anticoagulant effect of rHV2. The rHV2 solution was also tested as a control.

Determination of Inhibition of Platelet Aggregation. Platelet-rich plasma was prepared as described above, and the residue blood was centrifuged at 500*g* for 10 min to get platelet-poor plasma. The platelet aggregation rate (PAR) was determined by LG-Paper-II Coagulation & Aggregation Meter (Steellex Corporation, China). ADP was used as inducer.[38] The inhibition rate (IR) of platelet aggregation was calculated according to the following equation:

$$\mathrm{IR} = \frac{\text{PAR of blank blood} - \text{PAR of rHV2-loaded micelles or rHV2}}{\text{PAR of blank blood}} \times 100\%$$

Confocal Laser Scanning Microscopy. RGD−PEG-*g*-chitosan and mPEG-*g*-chitosan were labeled with FITC. Briefly, 50 mg of RGD−PEG-*g*-chitosan or mPEG-*g*-chitosan was added to 2 mL of acetone solution with 2.03 mg of FITC with gentle stirring. The reaction was continued for 4 h at room temperature in the dark. Then FITC labeled RGD−PEG-*g*-chitosan or mPEG-*g*-chitosan, i.e., RGD−PEG-*g*-chitosan-FITC or mPEG-*g*-chitosan-FITC was obtained after the free FITC was removed by dialysis with a dialysis membrane (MW cutoff = 12−14 kDa, Millipore Co. Ltd., USA) against distilled water.

Drug-free PIC micelles labeled with FITC were prepared as described above except 0.2 mg/mL of rHV2 solution was replaced by PBS (pH 7.4, 50 mmol/L). The platelet-rich plasma was obtained by centrifugation of rabbit venous blood containing 3.28% (w/v) sodium citrate (1:9, v/v, for sodium citrate solution and blood) at 72 g for 10 min. After 10 μL of the micelle solution was mixed with 100 μL of platelet-rich plasma followed by addition of 10 μL of ADP solution (10 μmol/L) for 5 min, the binding of drug-free PIC micelles labeled with FITC to platelets was examined by confocal laser scanning microscope (Leica SP2, Heidelberg, Germany).

Statistical Analysis. All data were expressed as mean ± SD (standard deviation) unless particularly outlined. The statistical significance of differences among more than two groups was determined by one-way ANOVA by the software SPSS 13.0. A value of $p < 0.05$ was considered to be significant.

Results

Synthesis and Characterization of mPEG-*g*-chitosan and RGD−PEG-*g*-chitosan. The conversion degree from hydroxy-group to aldehyde-group was 32% for mPEG and 40% for PEG, respectively. The synthesis of mPEG-*g*-chitosan was confirmed by ^{1}H NMR and FTIR. ^{1}H NMR: δ 4.35−3.64 (H-3, H-4, H-5, H-6), 3.53 (−OCH_2−), 3.29 (H-2), 3.21 (−OCH_3), 2.60 (−NH−CH_2−), 2.09 ppm

(35) Ban, E.; Ryu, J. C.; Yoo, Y. S. Detection of recombinant hirudin using capillary electrophoresis with laser-induced fluorescence detection. *Microchem. J.* **2001**, *70*, 211–217.

(36) Meng, M.; Liu, Y.; Wang, Y. B.; Wang, J. C.; Zhang, H.; Wang, X. Q.; Zhang, X.; Lu, W. L.; Zhang, Q. Increase of the pharmacological and pharmacokinetic efficacy of negatively charged polypeptide recombinant hirudin in rats via parenteral route by association with cationic liposomes. *J. Controlled Release* **2008**, *128*, 113–119.

(37) Fu, K.; Izquierdo, R.; Walenga, J. M.; Fareed, J. Comparative study on the use of anticoagulants heparin and recombinant hirudin in a rabbit traumatic anastomosis model. *Thromb. Res.* **1995**, *78*, 421–428.

(38) Fabre, J. E.; Nguyen, M.; Latour, A.; Keifer, J. A.; Audoly, L. P.; Coffman, T. M.; Koller, B. H. Decreased platelet aggregation, increased bleeding time and resistance to thromboembolism in P2Y1-deficient mice. *Nat Med.* **1999**, *5*, 1199–1202.

Table 1. Characterization of mPIC Micelles and RGD−PIC Micelles ($n = 3$)[a]

micelles	mean size (nm)	PDI	zeta potential (mV)	EE (%)
mPIC	30.9 ± 0.5	0.24 ± 0.004	1.855 ± 0.046	76.9 ± 0.84
RGD−PIC	41.9 ± 1.8**	0.28 ± 0.02	0.089 ± 0.499	81.1 ± 0.85*

[a] *$p < 0.01$, **$p < 0.001$ versus mPIC micelles.

(−$COCH_3$). The results were in accordance with those reported in the literature.[15,29] Further, the intensity of the peak at about 3400 cm^{-1} for amino groups in the FTIR spectrum decreased for the titled product compared with that of chitosan, which was attributed to the linkage of mPEG-CHO to some amino groups in chitosan. In addition, compared to the spectrum of chitosan, the peak of 2886 cm^{-1} (specific absorption peak of PEG) appeared in the spectrum of the titled product. These results implied that the aldehyde groups of mPEG-CHO were associated with amino groups of chitosan, which confirmed the successful linkage of mPEG-CHO to chitosan.

The ^{1}H NMR result of RGD−PEG-*g*-chitosan was just similar to that of mPEG-*g*-chitosan except for the absence of peak 3.21 (−OCH_3) due to the relatively low content of RGD in RGD−PEG-*g*-chitosan molecules. The FTIR spectrum of the title product also showed the presence of amino groups (decreased intensity of 3400 cm^{-1}) and PEG (2880 cm^{-1}). Nitrogen element analysis was hence first used to support the successful linkage of RGD with PEG due to the fact that there is no nitrogen atom in the PEG molecule and the free RGD was removed by dialysis. It was found that 20.03% of RGD was linked with PEG. In addition, the thin layer chromatography suggested the formation of RGD−PEG-*g*-chitosan (data not shown), in which the spots of amino acids and small amount of RGD were found for the hydrolysis product of RGD−PEG-*g*-chitosan, wherein the spots of RGD resulted from hydrolysis product of Schiff base which has not been reduced by $NaBH_3CN$. These results suggested that the title product was successfully obtained. The grafting degrees of chitosan for mPEG-*g*-chitosan and RGD−PEG-*g*-chitosan were 5.3% and 4.6% (mol/mol), respectively.

Characterization of PIC Micelles. The size and polydispersity data of mPIC micelles and RGD−PIC micelles are shown in Table 1. A typical representation of the DLS measurements is presented in Figure 2, and illustrates the narrowness of the size distribution of the PIC micelles. The size of mPIC micelles and RGD−PIC micelles was found to be 30.9 ± 0.5 nm and 41.9 ± 1.8 nm, respectively, indicating that the mean diameter of RGD−PIC micelles was significantly larger than that of mPIC micelles ($p < 0.001$). This might be attributed to the electrostatic repulsion of negatively charged RGD on the micelle surface. The nanoscaled size of micelles as well as the hydrophilic PEG palisade surrounding the core are important features of the PIC micelles to avoid their uptake by the reticuloendothelial system.

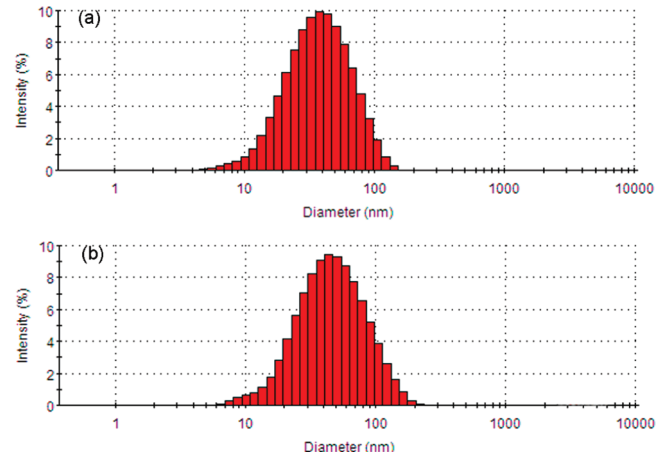

Figure 2. Size distribution of mPIC micelles (a) and RGD−PIC micelles (b).

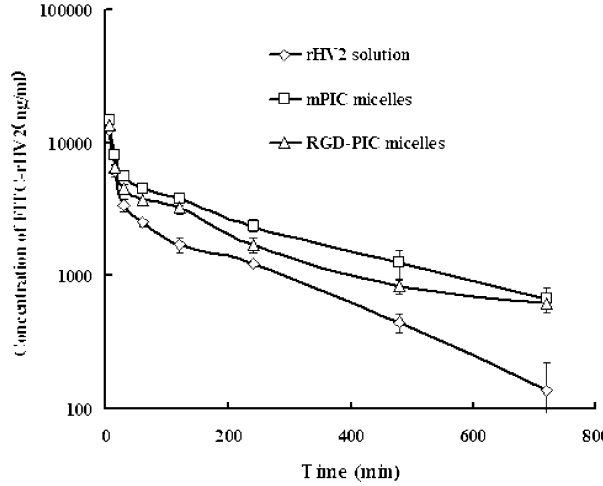

Figure 3. FITC-rHV2 plasma concentration−time profiles for different rHV2 formulations in rats ($n = 5$).

The EE estimated after ultrafiltration of the micelle solution was approximately 80% (Table 1), and the EE of RGD−PIC micelles was increased by about 4% compared with mPIC micelles although the significant difference in EE was found between the two micelles, which might be accounted for the size increase of RGD−PIC micelles compared with mPIC micelles.

As shown in Table 1, zeta potential of both PIC micelles was near 0 mV, suggesting that the micelles exhibited optimal stability owing to the complete charge neutralization leading to enhanced hydrophobic interaction in the core of micelles.[39]

Pharmacokinetics of PIC Micelles. The FITC-rHV2 plasma concentration−time profiles after intravenous administration of rHV2 solution, mPIC micelles and RGD−PIC micelles to rats are shown in Figure 3. After iv administration of rHV2 formulations (2 mg/kg), the C_0 value was near 20 μg/mL for all groups (Table 2). The plasma rHV2 level decreased distinctly in solution group, less than the effective

(39) Adams, D. J.; Rogers, S. H.; Schuetz, P. The effect of PEO block lengths on the size and stability of complex coacervate core micelles. *J. Colloid Interface Sci.* **2008**, *322*, 448–456.

Table 2. Pharmacokinetic Parameters of rHV2 for Different Formulations ($n = 5$)[a]

parameter	rHV2 soln	mPIC micelles	RGD−PIC micelles
AUC (min·μg/mL)	902.1 ± 40.1	1734.7 ± 118.2*[a]	1376.0 ± 96.9*[a,*b]
MRT (min)	160.7 ± 7.7	207.4 ± 19.2*[a]	198.1 ± 5.2*[a,**b]
C_0 (μg/mL)	19.7 ± 2.1	19.9 ± 2.8**[a]	19.7 ± 1.9**[a,**b]
CL (mL/min/kg)	2.2 ± 0.1	1.1 ± 0.1*[a]	1.4 ± 0.1*[a,*b]

[a] *$p < 0.05$, **$p > 0.05$ versus solution (a) and mPIC micelles (b).

blood level (1.67 μg/mL, obtained by APTT test as follows) after 2 h, whereas the effective blood levels of rHV2 for mPIC micelles and RGD−PIC micelles were maintained for 4 h and 6 h, respectively. In addition, it is worthy of special note that the plasma rHV2 level for RGD−PIC micelles was lower than that for mPIC micelles over the whole experiment period.

The pharmacokinetic parameters for rHV2 formulations are listed in Table 2. The AUC of mPIC micelles and RGD−PIC micelles were 1.9 and 1.5 times higher than that of solution ($p < 0.05$), respectively, and, noticeably, the AUC of mPIC micelles was significantly higher than that of RGD−PIC micelles ($p < 0.05$). The mean retention time (MRT) of rHV2 for both micelles was significantly prolonged ($p < 0.05$) compared with the solution, and the significant difference in MRT between the two micelles was not found ($p > 0.05$). The clearance rates (CL) of rHV2 for both micelles were significantly lower than that of rHV2 solution ($p < 0.05$), whereas the CL of rHV2 for RGD−PIC micelles was significantly higher than that of rHV2 for mPIC micelles ($p < 0.05$). Therefore, it was concluded that PIC micelles could significantly retard the clearance of rHV2 in blood to give higher blood levels as compared with rHV2 solution, especially for mPIC micelles, thus holding a significant advantage in favorable pharmacokinetic behavior of rHV2. These results are consistent with our previous report.[16]

Anticoagulant Activity of rHV2-Loaded PIC Micelles. APTT was often used to evaluate the pharmacological efficacy of thrombin inhibitor.[40,41] It was reported that chitosan was an effective inducer for platelet adhesion and aggregation[42] and accelerated blood clotting. Accordingly, APTT of mPEG-*g*-chitosan and RGD−PEG-*g*-chitosan polymer themselves were assayed, respectively. It was found that the percentage of changes (vs normal value) in APTT ranged from 97.7 ± 4.8% to 99.8 ± 2.0% for mPEG-*g*-chitosan and 96.7 ± 2.2% to 98.4 ± 1.7% for RGD−PEG-*g*-chitosan, respectively, within the concentration of 10 to 160 μg/mL, which corresponded to the equivalent concentration range of them used for APTT evaluation for rHV2-loaded mPIC micelles and RGD−PIC micelles, indicating that both of the copolymers could slightly decrease APTT.

Figure 4 showed the percentage of changes in APTT for mPIC micelles and RGD−PIC micelles. As compared with rHV2 solution, mPIC micelles decreased APTT of rHV2 when the concentration of rHV2 was lower than 9.0 μg/mL, and prolonged thereafter. As anticipated, RGD−PIC micelles

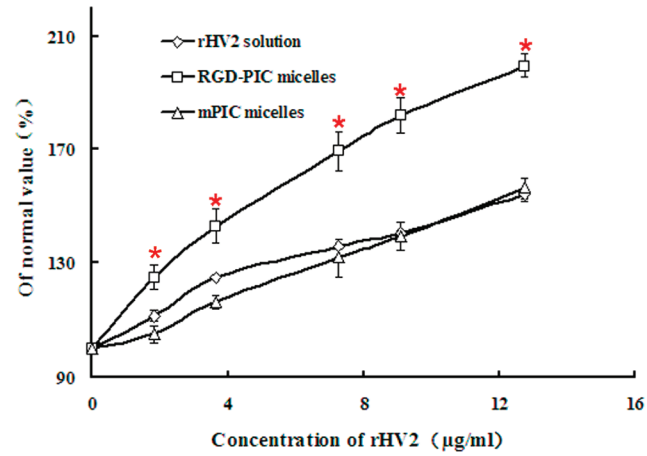

Figure 4. Relationship between percent of prolongation in APTT and rHV2 concentrations for different rHV2 formulations ($n = 3$) (*$p < 0.01$ versus mPIC micelles).

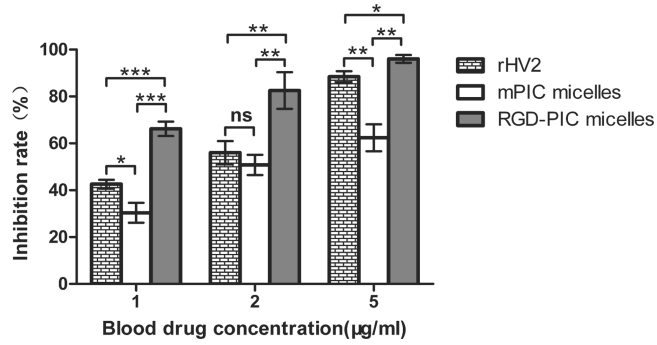

Figure 5. Inhibition rates of platelet aggregation for different rHV2 formulations ($n = 3$) (*$p < 0.05$, **$p < 0.01$, ***$p < 0.001$).

drastically prolonged APTT in the range of tested rHV2 concentrations, and APTT values of RGD−PIC micelles were significantly higher than those of mPIC micelles in the whole tested concentration range ($p < 0.01$).

Inhibition Rate of Platelet Aggregation of rHV2-Loaded PIC Micelles. As shown in Figure 5, the inhibition rate (IR) of platelet aggregation for different rHV2 formulations remarkably increased with the increase of rHV2 concentration. When the rHV2 concentration varied from 1 μg/mL to 5 μg/mL, the IR of RGD−PIC micelles increased from 66.2 ± 3.1% to 96.0 ± 1.6%, whereas the IR of rHV2 solution and rHV2-loaded mPIC micelles were 42.6 ± 1.9% to 88.5 ± 2.3% and 30.3 ± 4.2% to 62.4 ± 5.6%, respectively. Compared with rHV2 solution, rHV2-loaded mPIC micelles

(40) Salmela, B.; Albäk, A.; Räike, P.; Lepäntalo, M.; Lassila, R. A direct thrombin inhibitor, lepirudin, for thrombophilic patients with inoperable critical limb ischemia. *Thromb. Res.* **2009**, *123*, 719–723.

(41) Brodin, E.; Appelbom, H.; Øterud, B.; Hilden, I.; Petersen, L. C.; Hansen, J.-B. Regulation of thrombin generation by TFPI in plasma without and with heparin. *Transl. Res.* **2009**, *153*, 124–131.

(42) Chou, T. C.; Fu, E.; Wu, C. J.; Yeh, J. H. Chitosan enhances platelet adhesion and aggregation. *Biochem. Biophys. Res. Commun.* **2003**, *302*, 480–483.

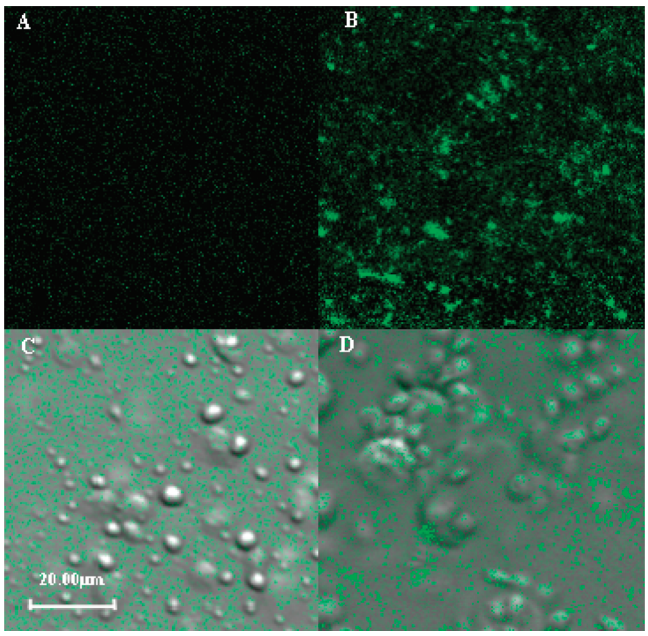

Figure 6. Confocal microscopic images of drug-free mPIC micelles labeled with FITC (A and C) and RGD−PIC micelles labeled with FITC (B and D).

exhibited significantly lower inhibition of platelet aggregation except rHV2 concentration was 2 μg/mL, whereas rHV2-loaded RGD−PIC micelles exhibited significantly greater inhibition of platelet aggregation. More importantly, RGD−PIC micelles had significantly higher inhibitory effect compared with mPIC micelles. These results were consistent with those of APTT test as described above and confocal microscope observation as described below.

Confocal Laser Scanning Microscopy Evaluation. In the case of our experiment, the platelet-rich plasma was used to evaluate the platelet targeting specificity of PIC micelles by observation with a confocal microscope. A homogeneous distribution in platelet-rich plasma for drug-free mPIC micelles labeled with FITC was observed in confocal images (Figure 6A and Figure 6C), indicating that mPIC micelles could not specifically bind to platelets. Expectedly, Figure 6B and 6D illustrated platelet-specific accumulation of drug-free RGD−PIC micelles labeled with FITC, suggesting that RGD−PIC micelles specifically bound to platelets. These results demonstrated platelet targeting specificity of RGD−PIC micelles.

Discussion

On one hand, nanotechnology will assume an essential place in drug delivery and human therapeutics.[43] There already exist a wide variety of nanoparticles such as polymeric micelles and liposomes, and diverse methods of synthesis have been developed. The pharmacokinetic parameters of these nanoparticles may be altered according to size, shape, and surface functionalization. Careful design of nanoparticle delivery agents will result in successful localization and drug delivery to specific biological targets coupled with the efficient evasion of the reticuloendothelial system. On the other hand, various thrombolytic agents such as rHV2 are associated with low thrombus specificity and short half-life, large dose required for clinical treatment and side effect of hemorrhage. Herein the platelet targeting PIC micelles which had specific affinity to activated platelets was designed to achieve long circulation in blood and release their contents after reaching the targeted site.

It is well-known that the driving force of PIC micelle assembly is the electrostatic interactions between the charged polymers and oppositely charged drugs. Therefore, PIC micelles were prepared in acidic buffered solutions (pH 5.0) to ensure that every amino group of the graft polymers was protonated, and rHV2 remained anionized in this condition due to its isoelectric point of 4.4.[44] When TPP solution was added into the mixture of rHV2 and mPEG-*g*-chitosan or RGD−PEG-*g*-chitosan, anions of TPP and rHV2 together interacted with chitosan cationic segment to form the core of PIC micelles via electrostatic interaction, and rHV2 was incorporated in the core during this process. Due to the electrostatic interactions between rHV2 and chitosan segments, the EE of PIC micelles with near electric neutrality were higher, up to about 80%. It could be seen that the micelle size was in the nanometer range and the size distribution was narrow.

There were several previous reports regarding the pharmacokinetics alteration of the drug encapsulated in polymeric micelles.[45,46] As shown in Figure 3, the rHV2 plasma concentration for PIC micelles was higher than that for rHV2 solution over the whole experiment period, suggesting that the *in vivo* release of rHV2 from PIC micelles was sustained, which led to the improvement of pharmacokinetic parameters of rHV2 loaded in PIC micelles, especially long circulation of rHV2 in blood. Importantly, it is worthy of special note that rHV2-loaded mPIC micelles exhibited better pharmacokinetic behavior compared with rHV2-loaded RGD−PIC micelles. This was in contrast to the result of the comparable *in vitro* release for both micelles (data not shown), and encouraging since it could assumably be attributed to the specific interaction of RGD with platelets. This interaction facilitated the selective localization of RGD−PIC micelles to platelets, thereby resulting in lowering the rHV2 level in plasma while maintaining a high rHV2 level in platelets compared with mPIC micelles. This result was in good agreement with those of *in vitro* pharmacodynamics (Figure

(43) Park, K. Nanotechnology: What it can do for drug delivery. *J. Controlled Release* **2007**, *120*, 1–3.

(44) Dette, C.; Wätzig, H. Separation of r-hirudin from similar substances by capillary electrophoresis. *J. Chromatogr., A* **1995**, *700*, 89–94.

(45) Vega-Villa, K. R.; Takemoto, J. K.; Yáñez, J. A.; Remsberg, C. M.; Forrest, M. L.; Davies, N. M. Clinical toxicities of nanocarrier systems. *Adv. Drug Delivery Rev.* **2008**, *60*, 929–938.

(46) Yang, X.; Li, L.; Wang, Y.; Tan, Y. Preparation, pharmacokinetics and tissue distribution of micelles made of reverse thermo-responsive polymers. *Int. J. Pharm.* **2009**, *370*, 210–215.

4 and Figure 5). Consequently, the results of pharmacokinetics also suggested that RGD−PIC micelles exhibited active targeting ability to platelets to a great extent in comparison with mPIC micelles as our previous report on liver-targeting PIC micelles.[15]

Previous study revealed that chitosan was an effective inducer for platelet adhesion and aggregation and its action mechanism may be associated, at least partly, with the increasing $[Ca^{2+}]_i$ mobilization and enhancing expression of GPIIb/IIIa complex on platelet membrane surface.[42] As a result, this unwanted action of mPEG-*g*-chitosan predominated in the lower rHV2 concentration, resulting in poor prolongation of APTT (Figure 4) and low inhibition of platelet aggregation rate (Figure 5) for rHV2-loaded mPIC micelles in comparison with rHV2 solution. Slower drug release from micelles might be another reason for these unexpected facts. More importantly, IR and APTT for rHV2-loaded RGD−PIC micelles were significantly greater than those for rHV2-loaded mPIC micelles and rHV2 solution. These could be attributed to the fact that the surface of rHV2-loaded PIC micelles was functionalized by RGD specifically binding to GP IIb/IIIa on the membrane of platelets, that is, rHV2-loaded RGD−PIC micelles possessed dual functions of platelets targeting and antiplatelets. On one hand, RGD on the surface of RGD−PIC micelles guided rHV2-loaded PIC micelles to localize on the platelets and herein rHV2 took effect. On the other hand, when blood coagulation started, GP IIb/IIIa on the membrane of platelets, the binding site to plasma fibrinogen, were activated.[47] If parts of binding sites on the activated platelets were occupied by RGD, the binding of the fibrinogen with platelets was partly inhibited,[48] thereby leading to the difficult formation of thrombus. Therefore, rHV2 inhibited the activity of thrombin in coordination with RGD. These results of *in vitro* anticoagulation and inhibition of platelet aggregation reinforced that RGD−PIC micelles could deliver more rHV2 to targeted platelets. This was also confirmed by intuitive observation of fluorescent imaging of the micelles with confocal microscope, which further demonstrated the platelet targeting specificity of RGD−PIC micelles. Micelle-forming materials were labeled with FITC to allow for precise fluorescent imaging of the micelles *in vitro*. The studies regarding *in vivo* platelet targeting effect will be carried out to fully characterize the nature of RGD−PIC micelles.

(47) Pollina, E. Design and Synthesis of RGD Mimetics as Potent Inhibitors of Platelet Aggregation. *J. Undergrad. Sci.* **1996**, *3*, 119–126.

(48) Jennings, L. K. Role of Platelets in Atherothrombosis. *Am. J. Cardiol.* **2009**, *103*, 4A–10A.

Conclusion

In summary, in use of graft copolymers of mPEG-*g*-chitosan and RGD−PEG-*g*-chitosan, mPIC micelles and RGD−PIC micelles with nanoscaled size and narrow size distribution were successfully prepared to incorporate rHV2 with high EE. It was proved that both mPIC micelles and RGD−PIC micelles displayed favorable pharmacokinetic characteristics in rats. The considerably higher AUC and MRT of rHV2 indicated that these micelles could greatly retard the clearance of rHV2 in blood. What's more, RGD-conjugated micelles appeared to significantly prolong APTT and enhance antiplatelet aggregation effect of rHV2 in comparison with mPIC micelles and rHV2 solution, suggesting that RGD−PIC micelles exhibited platelet targeting effect, which was confirmed by confocal imaging. Thus, RGD−PEG-*g*-chitosan is a promising polymer for preparing platelet targeting PIC micelles. It is expected that this novel nanocarrier may be practical for incorporation of other peptide and protein drugs.

Abbreviations Used

PIC, micelles polyion complex micelles; rHV2, recombinant hirudin variant-2; PEG, poly(ethylene glycol); mPEG, methoxy poly(ethylene glycol); mPEG-*g*-chitosan, methoxy poly(ethylene glycol)-grafted-chitosan; RGD, arginine-glycine-aspartic acid (Arg-Gly-Asp); RGD−PEG-*g*-chitosan, Arg-Gly-Asp-poly(ethylene glycol) grafted chitosan; mPIC micelles, mPEG-*g*-chitosan PIC micelles; RGD−PIC micelles, RGD−PEG-*g*-chitosan micellesTPP, pentasodium tripolyphosphate; EE, encapsulation efficiency; GP IIb/IIIa, globulin protein IIb/IIIa; FITC, fluorescein isothiocyanate; $NaBH_3CN$, cyanoborohydride; BCA, bicinchoninic acid; APTT, activated partial thromboplasmin time; TNBS, trinitrobenzenesulfonic acid; PDI, polydispersity index; DLS, dynamic light scattering; FITC-rHV2, FITC labeled rHV2; PBS, phosphate buffer solution; MRT, mean residence time; AUC, area under the plasma concentration−time curve up to last time; ADP, adenosine diphosphate; PAR, platelet aggregation rate; IR, inhibition rate; SD, standard deviation; CL, clearance rate.

Acknowledgment. We would like to acknowledge the support of this work by the National Development of Significant New Drugs (New Preparation and New Technology, 2009zx09310-001) and the National Basic Research Program of China (973 program, 2009CB930300).

MP900271R